Eur. Phys. J. Plus (2022) 137:537
https://doi.org/10.1140/epjp/s13360-022-02744-1

THE EUROPEAN PHYSICAL JOURNAL PLUS

Regular Article

Check for updates

Redshift systematics and the H_0 tension problem

S. Carneiro[1,2,a], **C. Pigozzo**[1,b], **J. S. Alcaniz**[3,c]

[1] Instituto de Física, Universidade Federal da Bahia, Salvador, BA 40210-340, Brazil
[2] PPGCosmo, CCE, Universidade Federal do Espírito Santo, Vitória, ES 29075-910, Brazil
[3] Observatório Nacional, Rio de Janeiro, RJ 20921-400, Brazil

Received: 24 February 2022 / Accepted: 20 April 2022

Abstract Recent studies have shown that a small systematic redshift error (z_g) of $\approx\ 10^{-4}$ in the type Ia supernovae (SNe) measurements can affect the estimates of cosmological parameters. Here, we show that it could also lead to a reduction of $\approx 5\%$ in the local value of the Hubble parameter H_0, when very low-z SNe are included in the fit of the magnitude-redshift data. The estimated value, $H_0 = 69.60^{+1.49}_{-1.58}$ km s^{-1} Mpc^{-1}, differs by $\approx\ 1.3\sigma$ from the latest CMB result from the Planck collaboration.

In the last few years, a significant discrepancy has been consolidated between the present values of the Hubble parameter (H_0) inferred from the observations of the cosmic microwave background (CMB) by the Planck collaboration [1,2] and from local measurements of the cosmic expansion using Cepheid variables and type Ia Supernovae (SNe) by the SH0ES collaboration [3,4]. The discrepancy, of $\approx 3.4\sigma$ in the SH0ES analysis of 2016 [3], has worsened to $\approx 4.4\sigma$ in their latest report of 2019 [4], and can reach $\approx 5.8\sigma$ when other late-time measurements of H_0 are combined, reinforcing what is currently known as the H_0-tension problem [5]. This cosmic discordance has motivated a number of studies on a possible solution to this problem which in general consider either extensions of the standard Λ—cold dark matter (ΛCDM) model (see, e.g. [6] for a recent review) or look for possible systematics in the calibration of Cepheid magnitudes that anchor the distance ladder to high-z SNe [7].

On the other hand, some analyses have consistently shown that a small systematic redshift error in the SNe measurements can affect the estimates of cosmological parameters (see, e.g. [8–10]). In a recent study, Calcino and Davis [10] fitted the JLA compilation [11] considering a homogeneous systematic error z_g as an extra free parameter alongside the usual cosmological parameters and found $z_g \approx (2.6^{+2.7}_{-2.8}) \times 10^{-4}$. Although compatible with zero, this positive mean value implies a higher value of the matter density parameter, i.e. $\Omega_{m0} \approx 0.313$, which is in good agreement with the CMB constraint on Ω_{m0} obtained from the Planck collaboration.

As also discussed in [10], the impact of such a value of z_g on the Hubble parameter determination from non-local SNe ($z > 10^{-2}$) is actually very small. For example, by fitting the SNe of Pantheon compilation [12] in the range $0.023 < z < 0.15$—the same interval used in the SH0ES H_0 analysis—the relative correction is $\approx 1\%$, as shown in Fig. 1. However, as shown below, a non-cosmological redshift component of the order of $z_g \approx 10^{-4}$ can impact the fitting of very low-z SNe ($z < 10^{-2}$), being significant enough to alleviate or even solve the H_0 tension. Clearly, the inclusion of this set of local SNe in the analysis demands the subtraction of the local flux and peculiar velocities, which would give rise to further systematics.

We circumvent this latter difficulty by considering here the following two-step approach:

1. First, we use the SH0ES values of distance modulus and H_0 given in [3] to determine the *uncorrected* redshift z^* of the 19 low-z SNe used in the intermediate step of their distance ladder building. The *corrected* cosmological redshift z is given by $(1 + z^*) = (1 + z)(1 + z_g)$.
2. Then, we use the resulting set of magnitude-redshift data points to determine the local Hubble parameter.

The data set used in our analysis is taken from Table 5 of [3]. Combining the peak SNe magnitudes (m_B^0) to the intercept of their Hubble diagram (a_B), we have

$$Y \equiv m_B^0 + 5a_B\ , \tag{1}$$

where

$$a_B = \log\left(cz\left\{1 + \frac{1}{2}\left[1 - q_0\right]z - \frac{1}{6}\left[1 - q_0 - 3q_0^2 + j_0\right]z^2\right\}\right) - 0.2\,m_B^0, \tag{2}$$

S. Carneiro, C. Pigozzo and J. S. Alcaniz have contributed equally to this work.

[a] e-mail: saulo.carneiro.ufba@gmail.com (corresponding author)
[b] e-mail: cpigozzo@ufba.br
[c] e-mail: alcaniz@on.br

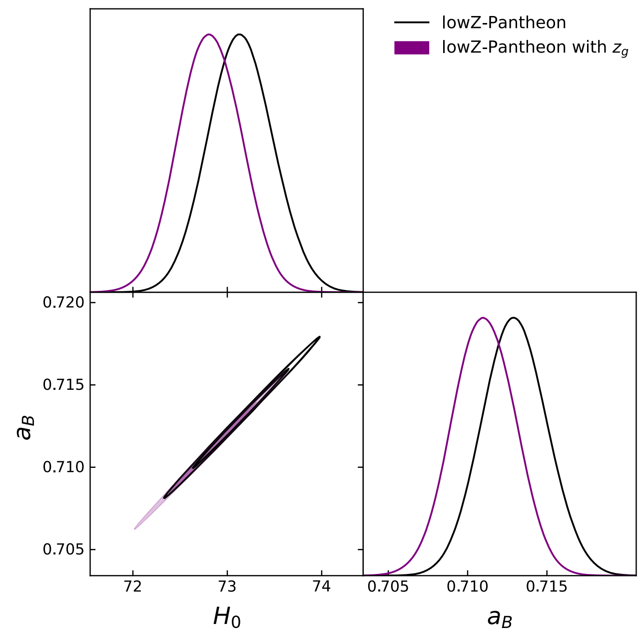

Fig. 1 Likelihoods for H_0 and a_B (defined in (2)) from the low-z Pantheon SNe [12] for uncorrected redshifts (black line) and when $z_g = 2.6 \times 10^{-4}$ is taken into account (magenta). The absolute magnitude was fixed as $M_B = -19.244$ [13]

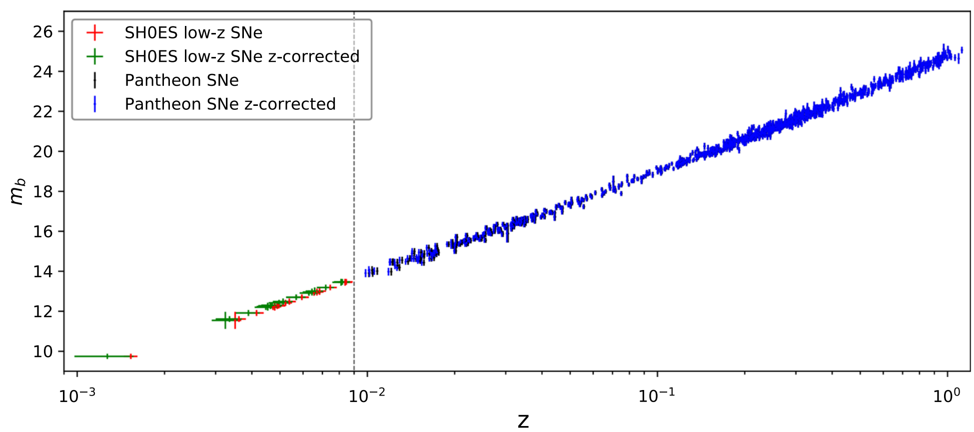

Fig. 2 Hubble diagram for corrected and uncorrected redshifts. The 19 low-z SNe (red and green points) are taken from Table 5 of [3], whereas the high-z data ($z > 10^{-2}$) correspond to the Pantheon compilation [12]

that is,

$$Y = 5\log\left(cz\left\{1 + \frac{1}{2}\left[1 - q_0\right]z - \frac{1}{6}\left[1 - q_0 - 3q_0^2 + j_0\right]z^2\right\}\right) \ , \tag{3}$$

with q_0 and j_0 being the usual deceleration and jerk parameters, respectively.

Assuming $q_0 = -0.55$ and $j_0 = 1$ [3], we use the values of Y given in [3] and Eq. (3) to first obtain the uncorrected cosmological redshift z_i^* for each one of the 19 low-z SNe of this subsample, with the corresponding errors given by $\sigma_{z_i^*} = \left[\frac{\partial Y}{\partial z}(z = z_i^*)\right]^{-1} \sigma_{Y_i}$. Then, considering a non-cosmological redshift correction, $z_g \approx (2.6^{+2.7}_{-2.8}) \times 10^{-4}$ [10], we determine the values of the corrected z_i. The resulting Hubble diagram considering *corrected* and *uncorrected* redshifts is shown in Fig. 2. Although small, the z_g correction is non-negligible and slightly changes the slope of the magnitude-redshift relation. For illustration, we also show the high-z SNe of the Pantheon compilation [12] .

In order to estimate H_0 from this low-z SNe sample, we perform a standard fitting procedure to maximise the likelihood function $\mathcal{L} \propto \exp(-\frac{1}{2}\chi^2)$, with

$$\chi^2\left(H_0\right) = \sum_i \left(\frac{\mu_{0,th}(z_i) - \mu_{0i}}{\sigma_{t,i}}\right)^2 , \tag{4}$$

where

$$\mu_{0,th}\left(z\right) = Y\left(z\right) + 25 - 5\log\left(H_0\right) \ . \tag{5}$$

The values of μ_{0i}, determined with the help of companion Cepheids, are also given in Table 5 of [3], and the total error in the denominator is given by $\sigma_{t,i}^2 = \sigma_{\mu_{0i}}^2 + \sigma_{\mu_{th}}^2$. By setting $z = z^*$, the analysis returns the uncorrected value of H_0 with $\sigma_{\mu_{th}} = \frac{\partial Y}{\partial z}(z =$

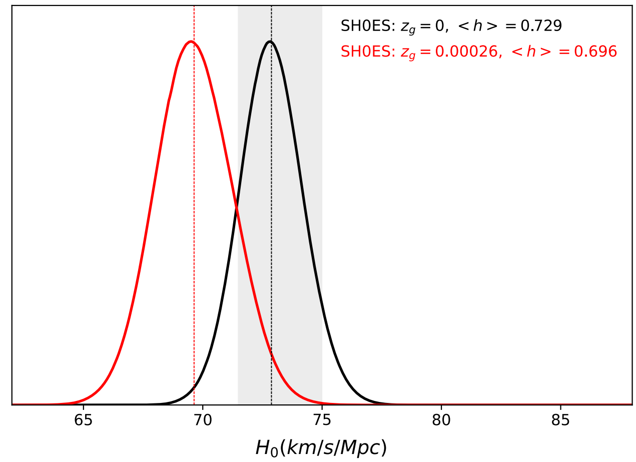

Fig. 3 Likelihoods for H_0 from local supernovas for uncorrected redshifts (black line) and when $z_g = 2.6 \times 10^{-4}$ is subtracted (red line)

Table 1 Comparison between the 19 low-z SNe Ia redshifts derived from the Riess et al. [3] best-fit for H_0 and the actual measured redshifts contaminated with the local flux and peculiar velocities

Host	Derived z	z (helio)	z (cmb)
M101	0.00152991	0.0008	0.0012075
N1015	0.00838253	0.00877	0.00800887
N1309	0.00744538	0.00713	0.00661791
N1365	0.00415132	0.00546	0.00513355
N1448	0.00472709	0.0039	0.00367588
N2442	0.00489259	0.00489	0.00528366
N3021	0.006704	0.00514	0.0060175
N3370	0.00654916	0.00427	0.00538706
N3447	0.00594548	0.00356	0.00468658
N3972	0.00538239	0.00284	0.00340569
N3982	0.00479261	0.0037	0.00426628
N4038	0.00479701	0.00548	0.00666127
N4424	0.00349949	0.00146	0.00258179
N4536	0.00360884	0.00603	0.00717496
N4639	0.0052243	0.0034	0.00446309
N5584	0.00594548	0.00546	0.00629435
N5917	0.00684365	0.00635	0.0069348
N7250	0.00495357	0.00389	0.00288199
U9391	0.00845573	0.00638	0.00665127

$z^*)\sigma_{z^*} = \sigma_Y$, whereas considering $z = z^* - z_g$, in order to find the *corrected* value of H_0, the distance modulus error must be replaced by $\sigma_{\mu_{th}} = \frac{\partial Y}{\partial z}(z = z^* - z_g)\sqrt{\sigma^2_{z^*} + \sigma^2_{z_g}}$. In both cases, a SALT-II systematic of 0.1 is added in quadrature [3].

The results of our analysis are shown in Fig. 3. The black line corresponds to the *uncorrected* data, while the red line represents the likelihood when a systematic correction $z_g = (2.6 \pm 2.8) \times 10^{-4}$ is subtracted. For the former case, our analysis furnishes $H_0 = 72.88^{+1.32}_{-1.28}$ km s^{-1} Mpc^{-1}, which is in 99.5% agreement with the value derived by the SH0ES team using 217 SNe Ia in the redshift interval $0.023 \leq z \leq 0.15$ [3]. Using the *corrected* data, we obtain $H_0 = 69.60^{+1.49}_{-1.58}$ km s^{-1} Mpc^{-1}. In this last case, the tension with the Planck 2018 value 67.36 ± 0.54 km s^{-1} Mpc^{-1} [2] is reduced to $\approx 1.3\sigma$.

Two important aspects are worth mentioning: first, that our analysis uses the sample of 19 nearby SN mentioned above irrespective of their role in the calibration of the distance ladder performed in [3]; second, that their *uncorrected* redshifts were not measured, but obtained by using the H_0 value determined in [3] and the known distances to their Cepheid companions. As mentioned earlier, this procedure is necessary in order to avoid the effects of a local flux and peculiar velocities, effects that are evidenced in Table 1. Indeed, we can see that, from the 19 local supernovas in the table, 14 presents a difference of order 10^{-3} between the simulated redshift and that measured in the CMB frame. For the remaining 5 supernovas, this difference has the order 10^{-4}, the same order of the redshift systematic we are treating here. On the other hand, the inclusion of local SNe in the Hubble constant determination

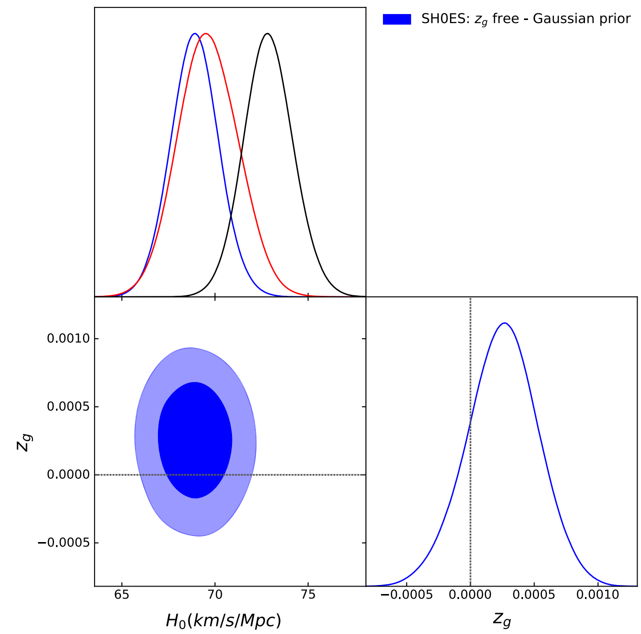

Fig. 4 Confidence regions for z_g and H_0 from the fitting of the Riess et al. [3] 19 low-z SNe Ia, assuming a prior on z_g discussed in the text (blue lines). The black line corresponds to the *uncorrected* data, whereas the red line to the data *corrected* with z_g reported by [10]

is necessary if one wants to find its actual local value. Although the redshift systematic of distant supernovas leads to only 1% correction in the Hubble constant value (see Fig. 1), when local SNe are included the correction grows to 5%, as we have shown. The essential reason is that the $z \times \mu$ curve has to necessarily cross the origin of the Hubble diagram. With only distant supernovas, this constraint is not important and the correction of the systematic leads to a simple vertical shift of the curve. When local SNe are included, however, this constraint leads to a sensible shift in the slope of the curve and to a larger correction to H_0 (see Fig. 2).

For completeness, we show in Fig. 4 the confidence regions for z_g and H_0 when z_g is free to vary in the interval $z_g \in [-0.01, 0.01]$, imposing the value found in [10] as a Gaussian prior. Although the fitting procedure involves only 19 low-z supernovae, we obtain an interval for z_g comparable to that obtained with the full JLA sample of high-z SNe. This is remarkable if we remind that our fitting analysis constrains z_g and H_0, whereas in [10] the constrained parameters are z_g and Ω_{m0}.

The origin of a redshift systematics, if genuine, demands for further investigation. Wojtak et al. [9] estimated the gravitational redshift component owing to the local potential well as $z_g \sim -10^{-5}$, which is too small to account for the Hubble tension and with opposed sign, indicating the presence of a local void. Other possible sources of redshift errors were discussed in [14]. It is noteworthy that the systematics found in [10] is in remarkable agreement with the gravitational redshift caused by white dwarfs, SNe Ia progenitors. Indeed, the maximum radius of a white dwarf with Chandrasekhar mass $M \approx 1.4\, M_\odot$ is $R \approx 0.01\, R_\odot$, which gives a lower limit for the gravitational redshift $z_g \approx 1.4 \times 10^{-4}$. However, redshifts are mostly measured from host galaxies, for which no relevant gravitational redshift is usually expected. Nevertheless, gravitational redshift can affect light emitted from the galactic bulges if they are inhabited by super-massive black holes. For a central black hole of 10^8 solar masses, the light emitted from $\approx 10^{-2}$ pc from its centre—a typical radius of broad-line regions [15]—has $z_g \approx 10^{-4}$. Although it has the order of aleatory errors in redshift measurements, this systematic may affect the determination of cosmological parameters, as discussed here and in other recent studies.

Finally, it is worth mentioning that solutions for the H_0 tension spam a wide class of non-standard cosmological models or modified gravity theories, as summarised, e.g. in [16] and [17]. In these studies, the present status of different observational probes at early and late epochs is also discussed and compared, evidencing the increasing tension not only in H_0 but also, at a lower level, in other cosmological parameters like the amplitude of matter perturbations σ_8. The next decade will testify a remarkable precision in measurements of cosmological parameters, specially with the accumulation of gravitational wave events, which will be able to determine H_0 with great precision (see, e.g. [18, 19]). In this context, systematic errors like the ones discussed here may be relevant before arguing in favour of exotic solutions, as they can potentially alleviate the tensions to acceptable levels.

Acknowledgements We are thankful to J. A. de Freitas Pacheco and J. Chaves-Montero for helpful comments and discussions. SC is supported by CNPq with Grant No. 311584/2020-9. JSA acknowledges support from CNPq (Grants Nos. 310790/2014-0 and 400471/2014-0) and FAPERJ (Grant No. 204282).

Data Availability Statement The data that support the findings of this study are openly available in [3]. This manuscript has no associated data or the data will not be deposited. [Authors' comment: There are no associated data available.]

References

1. P.A.R. Ade et al., A&A **571**, A16 (2015)
2. N. Aghanim et al., A&A **641**, A6 (2020)
3. A.G. Riess et al., Astrophys. J. **826**, 56 (2016)
4. A.G. Riess, S. Casertano, W. Yuan, L.M. Macri, D. Scolnic, Astrophys. J. **876**, 85 (2019)
5. L. Verde, T. Treu, A.G. Riess, Nat. Astron. **3**, 891 (2019)
6. E. Di Valentino, O. Mena, S. Pan, L. Visinelli, W. Yang, A. Melchiorri, D.F. Mota, A.G. Riess, J. Silk, Class. Quant. Grav. **38**, 153001 (2021)
7. G. Efstathiou. arXiv:2007.10716 [astro-ph.CO]
8. A. de Lavallaz, M. Fairbairn, Phys. Rev. D **84**, 083005 (2011)
9. R. Wojtak, T.M. Davis, J. Wiis, JCAP **1507**, 025 (2015)
10. J. Calcino, T.M. Davis, JCAP **1701**, 038 (2017)
11. M. Betoule et al., A&A **568**, A22 (2014)
12. D.M. Scolnic et al., Astrophys. J. **859**, 101 (2018)
13. G. Efstathiou, MNRAS **505**, 3 (2021)
14. T.M. Davis, S.R. Hinton, C. Howlett, J. Calcino, MNRAS **490**, 2948 (2019)
15. B. Czerny, K. Hryniewicz, A&A **525**, L8 (2011)
16. E. Di Valentino et al., Astropart. Phys. **131**, 102605 (2021)
17. E. Di Valentino et al., Astropart. Phys. **131**, 102606 (2021)
18. H.-Y. Chen, M. Fishbach, D.E. Holz, Nature **562**, 545 (2018)
19. J.M.S. de Souza, R. Sturani, J.S. Alcaniz, JCAP **2203**, 025 (2022)